Phase diagram, thermodynamic properties and long-term isothermal stability of quaternary molten nitrate salts for thermal energy storage

Alexander Bonk[1, a)] and Markus Braun[1] and Thomas Bauer[2]

[1]*German Aerospace Center (DLR), Institute of Engineering Thermodynamics, 70569 Stuttgart, Germany*
[2]*German Aerospace Center (DLR), Institute of Engineering Thermodynamics, 51147 Köln, Germany,*
[a)]Alexander Bonk: alexander.bonk@dlr.de

Keywords: thermal stability, molten salt, concentrating solar power (CSP), heat transfer fluids (HTF)

Abstract

Thermal energy storage (TES) is a vastly growing technique that allows for the generation of dispatchable electricity in modern concentrating solar power (CSP) plants. In solar tower systems the key to success is the use of a heat transfer fluid (HTF) and storage medium known as Solar Salt. This nitrate salt mixture of $NaNO_3$ and KNO_3 is considered thermally stable, non-toxic and environmentally friendly. In line-focusing CSP plants Solar Salt is still not being used as heat transfer fluid due to the inherent risk of freezing and related systematic failure. Accordingly, there is a need to develop nitrate salts with lower melting temperatures but yet acceptably high thermal stability. The information on molten nitrate mixtures with low melting points ($\lessapprox$100 °C) is limited, especially in terms of isothermal stability tests. This work presents thermo-physical data of the complex quaternary Ca,Li,Na,K//NO_3 system. Melting temperatures of more than 100 mixtures were assessed and compositions with melting points below 100 °C were identified. The heat capacity of selected mixtures was in the range of 1.5-1.6 kJ/kg K and generally increased with increasing Li-content. Thermal stability, with Solar Salt as reference salt, indicated that the stability of all mixtures did not exceed 500 °C but that the achievable ΔT was 360 °C, about 90 °C higher than that of Solar Salt. Some compositions are therefore are potential HTF and storage media but the overall Ca-content plays a crucial role in the decomposition of the quaternary mixtures during operation at high temperatures.

Introduction

Molten nitrate salts are used as heat transfer fluids (HTF) and storage media in modern concentrating solar power (CSP) plants.(Bonk et al., 2018; González-Roubaud et al., 2017; Reddy et al., 2013; Vignarooban et al., 2015) In new types of line-focussing CSP plants with molten salt as heat transfer fluid the ubiquitous risk of salt freezing led to the development of salt systems based on nitrate and/or nitrite salts that exhibit lower melting temperatures than conventionally used Solar Salt.(Bauer et al., 2013) Specific salt candidates that have been investigated in the past are HitecXL (Siegel et al.) (eutectic in the Ca,Na,K//NO_3-system), Hitec (eutectic in the Na,K//NO_2,NO_3-system) (Kirst et al., 1940) or eutectics in the Li,Na,K//NO_3 (abbreviated as LiNaK) – system (Siegel et al.). The authors of this work recently reviewed and discussed thermo-physical properties of these mixtures in terms of melting points, heat capacity, density, viscosity and thermal stability.(Bonk et al., 2018)

Table 1 Eutectic and most important non-eutectic salt systems based on nitrate and nitrite salts, their eutectic composition, melting points (liquidus temperatures) and maximum temperature stability.

	Composition [wt%]							T_m [°C]
Salt System	**$Ca(NO_3)_2$**	**KNO_3**	**$NaNO_3$**	**$LiNO_3$**	**$NaNO_2$**	**$LiNO_2$**	**KNO_2**	
Na/K//NO_3	-	40	60	-	-	-	-	~240
Solar Salt†	-	55	45	-	-	-	-	220
K,Li//NO3 (Carveth, 1898)		65	-	35	-	-	-	132
Na,Li//NO3 (Lehrman and Breslow, 1938)	-	-	50.4	49.6	-	-	-	192
Ca,Li//NO3 (Lehrman et al., 1937)	30	-	-	70	-	-	-	235
Ca,K//NO3 (Protsenko and Bergman, 1950)	61.97	38.03	-	-	-	-	-	146
Ca,Na//NO3 (Protsenko and Medvedev, 1963a)	62.7	-	37.3		-	-	-	226
K/Na/Li//NO_3 (Siegel et al.)	-	45	18	37	-	-	-	120
Ca/Na/Li//NO_3 (Lehrman and Breslow, 1938)	29.5	-	40	30.5	-	-	-	170
Ca/K/Li//NO_3 (Lehrman et al., 1937)	15	62	-	23	-	-	-	117
K,Na//NO_2/NO_3 (Berul and Bergman, 1954)	-	53	7	-	40	-	-	142
Li,Na//NO_2,NO_3 (Protsenko and Medvedev, 1963b)	-	-	43	-	13	44	-	126
K,Li//NO_2,NO_3 (Protsenko and Shisholina, 1963)	-	11.2	-	14.8	-	40.4	33.6	94
Ca/K/Na/Li//NO_2,NO_3	13.6			24.6	16.8	-	45	71
†: non-eutectic mixture								

It could be concluded that all candidates exhibit lower melting points than Solar Salt, but there is still a potential for a significant advance towards melting temperatures below 100 °C. Complex systems such as the quaternary Ca/K/Li/Na//NO_3 or the quinary reciprocal Ca/K/Li/Na//NO_2,NO_3 (Bonk et al., 2018) are likely to further reduce the melting temperatures compared to the HitecXL or LiNaK salt. A list of the most relevant eutectic (and one non-eutectic) compositions from known binary, ternary, quaternary and quinary reciprocal salt systems based on alkaline and earth-alkaline metal nitrates and nitrites is shown in Table 1.

Available phase diagrams of relevant nitrate salt systems

The melting and crystallization behaviour of a salt mixture must be understood to consider its suitability as TES and HTF medium. Significant effort has been put into understanding phase transitions in nitrate salts for more than a century.(Bergman et al., 1955; Carveth, 1898; Kofler, 1955) In 1898, Carveth (Carveth, 1898) indicated that the $NaNO_3$-KNO_3 system is simply eutectic while e.g. Kofler (Kofler, 1955) found the formation of mixed crystals during cooling indicating the presence of a non-eutectic system. More precisely, thermo-microscopy measurements indicated that the solidus curve is slightly shifted from the liquidus curve and mixed crystals (referred to as Type III Roozeboom crystallization (Roozeboom, 1904)) form upon cooling the lowest melting mixture, rather than a homogenous crystal which would be the case for a eutectic mixture. Despite the discrepancy in terms of crystallization phenomena, both agreed on the composition (55-45 wt% KNO_3-$NaNO_3$) and melting point (221 °C - 222 °C) of eutectic $NaNO_3$-KNO_3.

Carveth also investigated the more complex ternary K,Li,Na//NO_3 system in the same publication mentioned earlier and indicated the presence of a eutectic composition with a crystallization temperature of 120 °C.(Carveth, 1898) The ternary systems, Ca,K,Li//NO_3 (Lehrman et al., 1937), and Ca,Li,Na//NO_3 (Lehrman and Breslow, 1938) were evaluated by Lehrman more than 3 decades later; in 1937 and 1938, respectively, followed by the evaluation of the Ca,K,Na//NO_3 system by Bergman (Bergman et al., 1955) in 1955, which was re-assessed by Gomez and co-workers more recently (Gomez et al., 2013).

For the K,Li,Ca/NO_3 system Lehrman and co-workers (Lehrman et al., 1937) used a furnace containing a snug-fit cylindrical copper block with three holes: two for pyrex tubes, one containing the sample and one containing shredded asbestos as reference material, and one smaller well for a thermocouple. The temperature difference between the sample and the asbestos reference (referred to as ΔT in Lehrman's work) were recorded using potentiometric methods.(Lehrman et al., 1936) Different methods were used to determine the melting points of the ternary K,Li,Ca/NO_3 system, depending on the degree of supercooling. In case of no supercooling, samples were heated above the melting point and slowly cooled and the time-ΔT plots were used to identify transition points and eutectic temperatures. This method was referred to as *cooling* method. Samples with a high degree of supercooling, were heated

very slowly until the last crystals disappeared visually, which is why Lehrman et al. refer to it as the *visual* method. When looking into the reports on the ternary (K,Na)Li,Ca/NO_3 systems ((Lehrman et al., 1937; Lehrman and Breslow, 1938)) more closely, it is obvious that supercooling always occurred in the calcium nitrate region where it was necessary to, quote: “inoculate with very fine crystals in order to prevent the formation of supercooled glasses which when formed did not crystallize on long standing”(Lehrman et al., 1937). Also, the region close to 100% calcium nitrate was not investigated in both ternary systems as “calcium nitrate decomposes before it melts”. Recent descriptions of more complex systems such as the Ca,Na,K//NO_3 system have been presented, e.g. by Gomez et al. (Gomez et al., 2013) The authors described phase transitions including invariant reactions (eutectoid/peritectoid and eutectic/peritectic), liquidus temperatures and solid-solid phase transitions in the ternary salts. With all that said it could be concluded that the cation type and composition can drastically affect the melting and crystallization behaviour in terms of invariant reactions and liquidus temperatures. Especially for multi-component salts containing calcium, supercooling phenomena were observed making the evaluation of the liquidus temperatures difficult. Cooling methods were often replaced by heating methods to determine transition temperatures, which has been adapted in this work.

The tetrahedral Ca,K,Li,Na//NO3 system

The four ternary systems create the sides of the tetrahedral Ca,K,Li,Na//NO_3 system and are plotted in Figure 1. Known compositions of the quaternary system Ca/K/Na/Li//NO_3, investigated in terms of melting properties by different authors, are presented Table 2. A phase diagram of the quaternary system has however not been presented to date and it is attempted to present a majority of the missing data in this work.

Table 2 Quaternary mixtures investigated in the available literature. Compositions are reprinted using the same decimal numbers as in the original publications.

Composition [mol%]					
KNO_3	$NaNO_3$	$LiNO_3$	$Ca(NO_3)_2$	T_{liq} (°C)	REF
47	16	25	12	< 95	(Cordaro and Bradshaw, 2010)
50	11	27	12	< 95	
49	14	20	17	< 95	
43	17	35	5	< 110	(Bradshaw, 2010)
41	16	33	10	< 110	
32	31	31	6	< 140	
30	30	30	10	< 140	
47	16	27	10	< 130	
45	15	25	15	< 120	
38	20	30	12	< 100	(Bradshaw, 2010; Cordaro and Bradshaw, 2010)
12.51	63.07	15.42	9.00	113.8	(Ahmad et al., 2017)
11.92	50.10	29.39	8.58	97.8	
11.39	38.29	42.12	8.20	97.1	
10.90	27.49	53.76	7.85	112.7	
11.92	50.10	29.39	8.58	118.8	
17.64	50.83	20.19	11.34	111.8	
21.96	44.31	29.78	3.95	122.6	(Ahmad et al., 2017; Ren et al., 2014)
24.62	37.62	31.72	6.04	117.8	
14.21	47.79	17.52	20.47	77	(Ren et al., 2014)
27.80	35.05	17.13	20.02	77	
24.52	51.53	15.11	8.83	121.60	
12.51	63.07	15.42	9.00	132.78	
11.92	50.10	29.39	8.58	123.20	
10.84	54.65	26.71	7.80	124.00	
13.98	58.74	17.23	10.06	128.20	

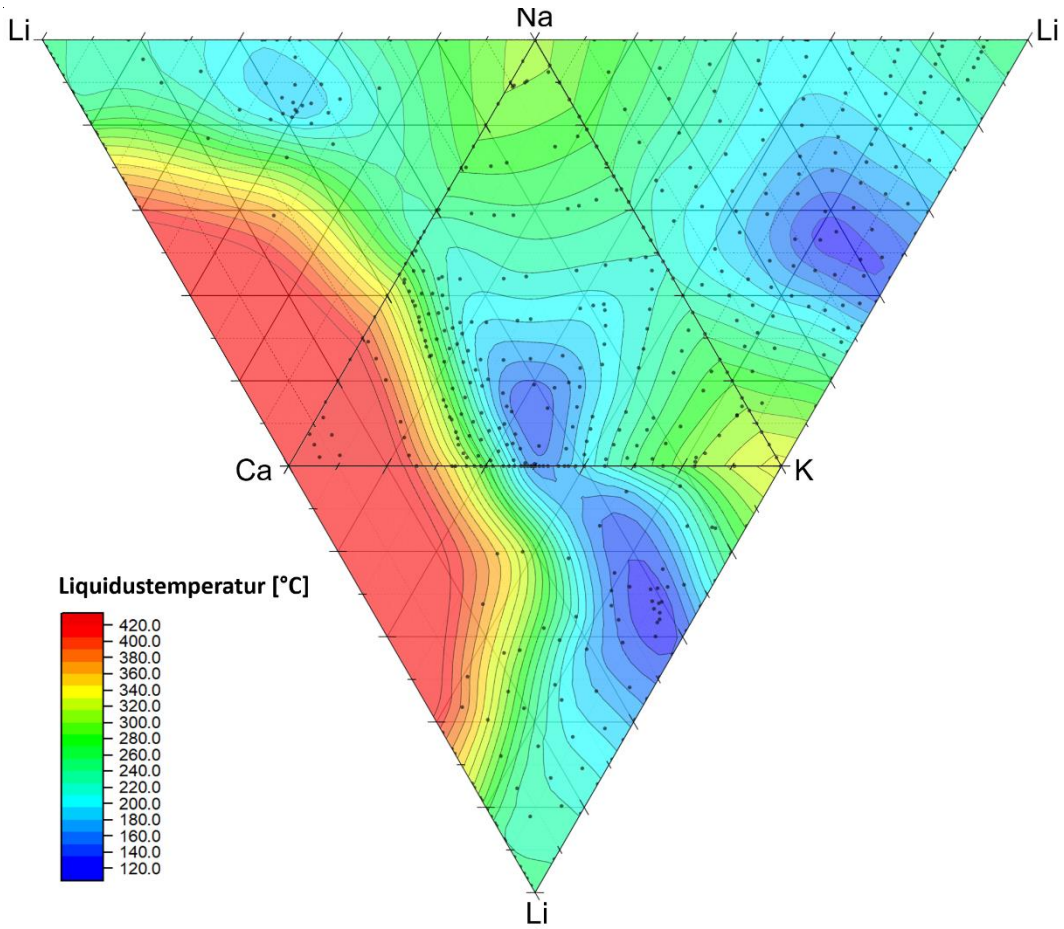

Figure 1 Combined phase diagrams of the ternary systems Ca,K,Na//NO_3 (Bergman et al., 1955), Ca,K,Li//NO_3 (Lehrman et al., 1937), Ca,Li,Na//NO_3 (Lehrman and Breslow, 1938), and K,Li,Na//NO_3 .The edges of each ternary diagram were taken from literature data of the binary systems K,Li//NO_3 (Carveth, 1898), Na,Li//NO_3 (Lehrman and Breslow, 1938), K,Na/NO_3 (Bale et al., 2016), Ca,K//NO_3 (Protsenko and Bergman, 1950), Ca,Na//NO_3 (Protsenko and Medvedev, 1963a) and Ca,Li//NO_3 (Lehrman et al., 1937). Data points are shown as black dots. Graphs were created using Origin(Pro) (Origin(Pro)) and contour lines were smoothened using a thin plate spline (TPS) algorithm (Donato and Belongie, 2002) (smoothing parameter = 0.05).

Thermal Stability of Molten Nitrate salts

Solar Salt, a non-eutectic mixture of sodium nitrate and potassium nitrate sets the benchmark as HTF and TES medium in the field of nitrate- based salt systems. The typical operating temperature range of Solar Salt is between 290 °C and 565 °C.(Kuravi et al., 2013) The upper temperature limit of the nitrate salt is restricted by equilibrium and/or decomposition reactions involving formation of nitrite (NO_2^-) and oxide ions (O^{2-}) according to eq (1) and (2).

$$NO_3^- \rightleftharpoons NO_2^- + \frac{1}{2}O_2 \quad (1)$$

$$2\,NO_2^- \rightleftharpoons O^{2-} + NO + NO_2 \quad (2)$$

While nitrite ions, formed by reaction (1), are known to affect the thermal properties of the melt (Bond and Jacobs, 1966; Bonk et al., 2017; Stern, 1972), oxide ions exacerbate corrosion and their formation is accompanied by the release of harmful nitrous gases (Baraka et al., 1975; M. De Jong and H. J. Broers, 1976; Zambonin, 1973).

The decomposition reactions (1) and (2) hold true for different nitrate salt systems. Chemical equilibria mainly depend on the exact cation type, composition of the mixture and the medium salt temperature. In general, the stability of the nitrate salt increases with decreasing charge density of the cation implying that nitrates of K^+, Na^+ and Li^+ are more stable than those of Ba^{2+}, Ca^{2+} or Mg^{2+}.(Yuvaraj et al., 2003) One of the few experimental works on quaternary nitrate salts based on Ca,K,Li,Na/NO_3 has been published by Cordaro and Bradshaw (Cordaro and Bradshaw, 2010) They filed a patent for multiple quaternary molten salts with crystallization temperatures below 95 °C (liquidus and solidification temperature are not used analogously in Cordaro's work). The high temperature limit was assessed by measuring the nitrite content (UV-Vis spectroscopy) of samples extracted from salt batches held at a defined temperature while dry air was bubbled through the melt. Cordaro and Bradshaw propose a thermal stability limit of "~520 °C" for three Ca/K/Li/Na mixtures which would be a significant increase of the applicable temperature range ΔT (= T_{max} - T_{min}) compared to Solar Salt. The same values were cited for another Ca,K,Li,Na//NO_3 mixture (12-38-30-20 wt%, respectively from ref. (Glatzmaier and Siegel, 2010)) by Delise *et al.* (Delise et al., 2019) for a thermodynamic assessment of different HTF.

Given that the minimum temperature is determined from the liquidus temperature plus a safety margin (+30 °C (Bonk et al., 2018)), the relevant ΔT of Solar Salt is 275°C whereas the ΔT of the quaternary salts of Cordaro's work would be 395 °C. The gravimetric storage capacity is approximately proportional to the mass, the heat capacity and the temperature difference (Q = m*cp* ΔT). Consequently, a large ΔT increases the gravimetric storage capacity of the salt. Given that the T_{min} and T_{max} values are suitable for the overall system, more compact storage configurations and further TES-cost reductions can theoretically be achieved. Yet, reliable high temperature limits from long-term isothermal test campaigns, the phase diagram and the heat capacity of the quaternary Ca,K,Li,Na,//NO_3 have not been presented to our best knowledge.

In this work the quaternary Ca,K,Li,Na,//NO_3 phase diagram, hereafter referred to as CaLiNaK, is assessed. The phase diagram is measured and expressed using ternary subsystems of the type $(Ca,Na,K)_{1-x}(Li)_x//NO_3$, each with a constant level of Li (x = 15 20, 25, 30, 35 mol%). Promising mixtures at different Li-concentrations are selected for further analysis in terms of heat capacity and finally thermal stability using dynamic thermogravimetry (TG) and isothermal (500 h) autoclave experiments. For autoclave experiments, the molten salt chemistry is derived using ion chromatography (IC) post-analysis of extracted samples. This method has proven successful in evaluating the molten salt chemistry in earlier studies.(Bonk et al., 2017; Bonk et al., 2018; Bonk et al.; Sötz et al., 2018) Decomposition reactions are discussed on the basis of these results and a final remark on the thermal stability of the CaLiNaK mixtures will be presented in comparison to conventional Solar Salt.

Theory

The melting point, maximum operating temperature and heat capacity are highly relevant properties for HTF and storage medium salt mixtures. Other relevant properties which are not in the focus of the present paper are the density, thermal conductivity and viscosity. These properties not only set the operation temperature limits of the attached power cycle but also determine the volumetric storage capacity, mass flows and dwell time in heat exchangers and receivers.

The melting point can be assessed using differential scanning calorimetry (DSC) methods. Even though test methods are known (e.g. ASTM E794), melting points are – confusingly enough – determined from the onset, peak maximum or sometimes the endset of melting, varying from author to author. To mention a few examples, Wu *et al*. (Yu-ting et al., 2017) used the onset of melting, Olivares (Olivares, 2012) and Fernandez *et al*. (Fernández et al., 2014) used the peak maximum, Raade and Padowitz (Raade and Padowitz, 2011) as well as Gomez (Gomez et al., 2013) used the endset (liquidus) to determine the melting points of different nitrate salts. In earlier studies by Lehrman *et al.* (Lehrman et al., 1937; Lehrman and Breslow, 1938) cooling methods based on differential-thermal, or sometimes optical methods, were used. In rare cases, e.g. when samples undergo supercooling, heating methods were used to identify the temperature at which the last solid residuals in the salt mixture disappeared. In summary, the varying interpretation of the melting peaks unfortunately leads to misinterpretation of transition temperatures throughout different publications. Hence, the following paragraph outlines the DSC theory and selects a suitable method for the present work.

The liquidus temperature, represented by the endset of the DSC melting peak, is of highest relevance for engineers since it represents the temperature at which a salt mixture is free of solid residues. The measured liquidus temperature depends on the melting enthalpy, heating rate, the sample mass and on the thermal resistances of the DSC-system.(2004) Typically, the liquidus temperature is therefore measured at various heating rates by DSC techniques and extrapolated to a heating rate of “0 K/min”. The onset of melting represents the solidus temperature and is almost independent of heating rate and sample mass. For congruently melting systems, this onset can be regarded as the eutectic melting temperature and it is (theoretically) identical to the onset of crystallization during cooling, which is typically also independent of cooling rate. Exceptions have to be made for samples with show signs of supercooling, where onset of melting and onset of crystallization can be delayed and occur spontaneously in some cases. The peak maxima in a DSC curve have less physical meaning and their position is affected by the melting enthalpy, heating rate, the sample mass and thermal resistances of the DSC system.

The heat capacity of molten salts is typically determined by DSC methods (e.g. ASTM E1269 (2017) or DIN 51007:2019-04) with errors of ± 3-10 %, e.g. as obtained in the frame of a round-robin test on the heat capacity of Solar Salt (Muñoz-Sánchez et al., 2017). The error is related to a number of parameters

that need to be controlled simultaneously. We have recently described the main influencing factors to be crucible specific (material, geometry, position in the DSC, lid), atmospheric conditions (flow rates, gas type), maximum temperature (creeping of the molten salt must be avoided), baseline stability / drift, the applied temperature profile, heat transfer within the heat transfer fluid (HTF) and storage medium sample, the type of reference and measuring system, methodology (e.g. ASTM E1269 and DIN 51007 differ slightly), but also "handling care" by the user (accuracy of preparation, cleanliness of the DSC system, exact and reproducible placement of crucibles on the sensor) (quoted from ref. (Bonk et al., 2018)). Accurate heat capacity measurements can only be obtained when controlling all parameters simultaneously.

The thermal stability of nitrate salts can be assessed using different methods and long term isothermal storage campaigns are ultimately the most reliable methods.(Bonk et al., 2018) This method is typically applied in a furnace with larger quantities of salts (50 g to a few kg) under a defined purge gas. Post-analysis of molten salts is typically used to determine the composition over time and conclude on the salt's stability under the given conditions. For molten nitrate salts however, salt creeping must be taken into consideration since it leads to significant mass loss and possibly contamination of infrastructure in the hot zone close to the crucible.

The alternative "3 % weight loss method", also known as *T3 method*, has first been employed by Raade and Padowitz (Raade and Padowitz, 2011) to qualitatively compare the decomposition temperatures of similar classes of molten salts. It has to be emphasized that the 3 % limit is a freely defined value. Although the authors explicitly state that the method is used for "screening purposes", it is often used for quantitative determination of decomposition temperatures of nitrate salts, which can lead to misleading results. It is also important to note that the T3 decomposition temperature is highly dependent on the heating rate (e.g. lower heating rates result in lower decomposition temperatures). In order to determine more precise decomposition temperatures lower heating rates would be required. However, there are different constraints with low heating rates (e.g. duration of measurement, salt creeping). Overall, it was found that the *T3 method* typically overestimates the long-term thermal stability limit of nitrate salts.(Bauer et al., 2013; Bonk et al., 2018)

Experimental Methods

Materials

For all experiments (DSC, TG-MS, Isothermal stability test) the quaternary Ca/K/Na/Li//NO_3 samples (hereafter referred to as CaLiNaK) were produced from stoichiometric weighing, mixing and mortaring of $NaNO_3$, KNO_3, $LiNO_3$ (all ≥ 99 %, Merck, Germany) and $Ca(NO_3)_2$*4 H_2O (≥99 %, Sigma Aldrich). For thermal analysis, samples were mixed before mortaring of around 0.5 g of each mixture for 5 to 10 minutes. All salt samples were homogenized by grinding in a pistil mortar and were allowed to absorb

moisture. This resulted in the formation of a homogeneous slurry of which around 25mg were transferred into an aluminum crucible. The crucible was successively placed in the DSC and heated to 250 °C (at a heating rate of 10 °C/min) for 20 minutes, leading to complete removal of absorbed moisture and crystal water. The DSC crucible was then sealed using an aluminum lid (cold welding), the lid was pierced and the crucible was ready for the actual DSC experiment. For a total of 40 samples the composition after DSC experiments was measured using ion chromatography (METROHM MODEL 883 BASIC IC PLUS) to confirm that the intended composition was identical to the experimentally gained composition and was not affected by the presence of moisture or crystal water.

Phase Diagram

To produce a phase diagram, the melting behaviour of a large number of compositions of the Ca/K/Na/Li//NO_3 system were measured in a NETZSCH DSC 204 PHOENIX F1, which was calibrated using Netzsch melting standards in a temperature range of 100 to 400 °C. Three successive measurement cycles were performed (typically between -40 °C and 250 °C) with samples containing ~15 mg of salt. The first DSC cycle was used for the removal of crystal water (short isothermal segment at 250 °C) followed by pre-melting and homogenization of the mixture. The second and third cycle typically yielded identical DSC curves indicating equilibrium conditions and only data of the subsequent second and third cycles are shown here. The same heating and cooling rates (10 K/min) were applied for all samples to allow a qualitative comparison of the liquidus temperatures of the tested samples. It should be noted that the "true" liquidus temperature (at an extrapolated heating rate of 0 K/min) is lower and that the presented liquidus temperatures are true for samples of 15 mg, heated at 10 K/min in aluminium crucibles. Different crucibles, samples masses and heating rates are likely to yield different results. For this configuration of crucible type, sample mass and heating rate, an indium standard exhibited a liquidus temperature of 158.7 °C, 160.2 °C and 161.4 °C at heating rates of 1, 5 and 10K/min, respectively. For this study, it is reasonable to assume that the real melting point of each mixture is around 3 °C lower than the value measured at 10K/min heating rate. Unlike in other studies, the cooling cycles were not used for determination of the liquidus temperature, because a number of samples showed severe supercooling (e.g. some samples did not solidify (or recrystallize) down to temperatures of -40 °C).

Heat Capacity

The heat capacity of selected samples was analyzed in the same NETZSCH DSC 204 F1 PHOENIX following the ASTM-E1269 (2017) in a temperature range of 50 °C to 350 °C. The procedure uses three consecutive measurements (all at 20 K/Min heating and cooling rate) of the blank aluminum crucible and lid (unpressed), crucible with lid and a sapphire reference (unpressed) and finally the identical crucible and lid with the molten salt sample (pressed and pierced). Multiple (identical) heating and cooling cycles were performed for each consecutive step and the first cycle was always neglected due to the presence of an endothermic dehydration peak.

Dynamic and isothermal stability tests

The qualitative decomposition temperature was investigated in a NETZSCH STA 449 TG following a similar procedure as the one applied by Raade and Padowitz.(Raade and Padowitz, 2011) Around 50 mg of sample were weighed into a platinum crucible without lid and heated to 250 °C (10 K/min) under N_2 (5.0 grade) atmosphere for 15 minutes to allow complete dehydration. Once steady state of the mass was reached, the sample was considered dehydrated and the following mass changes were attributed to decomposition reactions exclusively. The sample was heated to 700 °C with 10 K/min and the qualitative decomposition temperature under these dynamic was extracted at 3 % weight loss (*T3 method*, see ref.(Raade and Padowitz, 2011) for more detail).

For the isothermal stability tests around 100 g of each mixture were filled into a high purity alumina crucible and exposed to 500 °C for 500 h. Each crucible was purged with synthetic air (100 mL/min) and samples were extracted after 72, 120, 240, 408 and 500 h for chemical post-analysis. Those samples are referred to as "Bulk Salt" throughout this manuscript. A detailed description of the setup can be seen in ref. (Bonk et al., 2019).

Post analysis of molten salt samples involved the determination of anion and/or cation composition by anion chromatography (METROHM MODEL 883 BASIC IC PLUS), cation chromatography (METROHM MODEL 883 BASIC IC PLUS) and acid-base titration (METROHM TITRANDO 905). All of which techniques allowed for the qualitative and quantitative analysis of the anions: NO_3^-, NO_2^-, O^{2-}, CO_3^{2-}, and all alkaline and earth-alkaline metals. The exact procedures including an error analysis were previously described in more depth (Bonk et al., 2020; Bonk et al., 2017).

A list of compositions tested in terms of heat capacity and thermal stability (TG & Isothermal long-term tests) is provided in Table 3.

Table 3. Labels and respective compositions of formulations of the CaLiNaK phase diagram which were studied in more detail regarding heat capacity and thermal stability.

	Label	Composition [mol%]			
		K	Na	Li	Ca
Tested Compositions	**Li15**	45	15	15	25
	Li15-2	50	15	15	20
	Li20	42.5	12.5	20	25
	Li20-2	50	15	20	15
	Li25	52.5	12.5	25	10
	Li30	51.25	11.25	30	7.5
	Li35	52.5	10	35	2.5

Results & Discussion

Melting behaviour and phase diagram of the Ca/K/Na/Li//NO_3 system

Figure 2 exemplary DSC plots of formulation *Li30* (left) during the first and second heating and cooling cycle (both 10K/min). During the first heating cycle (solid lines) of the *Li30* sample one can observe two endothermic peaks and a liquidus temperature at (T_L) ~120 °C at a heating rate of 10 K/min. During subsequent cooling no exothermic crystallization peak is observed, indicating supercooling, and only around 0 °C a glass transition (T_g) seems to appear. In the second heating cycle of the *Li30* sample a pronounced exothermic peak (T_c) is detected with a maximum at 84.6 °C, which we ascribe to cold crystallization. It is followed by an endothermic melting peak with a liquidus temperature of 131 °C. Due the observed supercooling and cold crystallization phenomena we assume that the eutectic temperature (onset of melting) is hardly reliable, which is why liquidus temperatures (at 10 K/min) determined during heating were used to plot the phase diagram (or sub-phase diagrams) of the CaLiNaK system.

For the *Li35* sample (Figure 2 (right)) there is a crystallization peak during the first cooling segment (solid bottom line) with an onset (T_3) at 99.4 °C. In the subsequent (2^{nd}) heating cycle (dashed lines) an endothermic melting peak is detected with an onset (T_1) of 98.2 C. Since the onset of melting (T_1) and of crystallization (T_3) are very similar (99.4 °C and 92.6 °C, respectively) it is reasonable to assume that both represent eutectic melting temperatures. Therefore, the DSC curves of the *Li35* sample can be considered straight-forward while most of the other samples show signs of supercooling, which is indicated by the absence of a crystallization peak during cooling (*Li20-2*, *Li20*, *Li15-2* and *Li15* in Figure 3). Those samples did not show solidification even at temperatures as low as -40 °C.

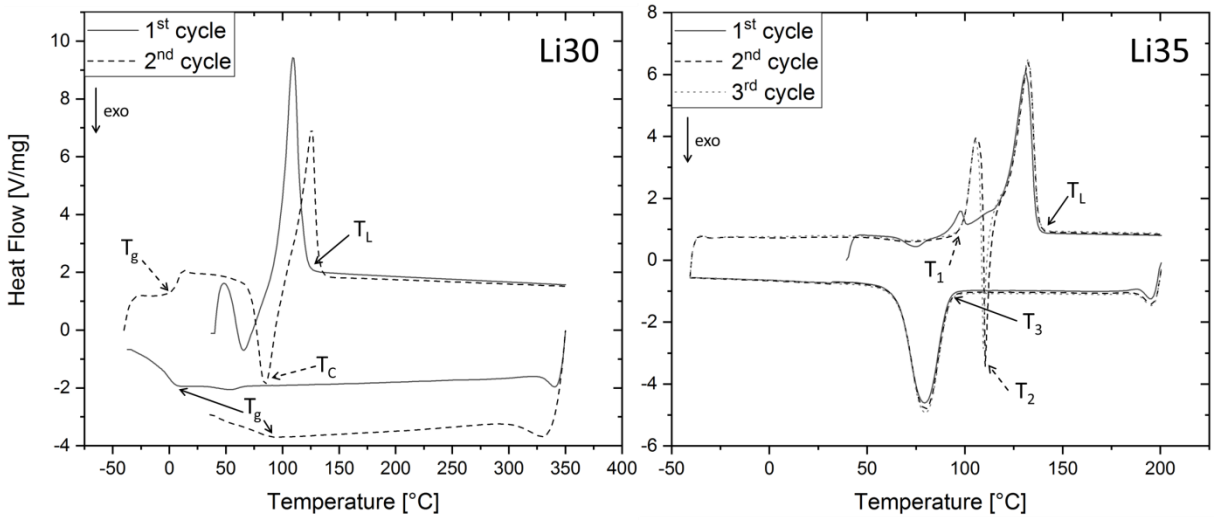

Figure 2. DSC plots of formulation *Li30* (left) and *Li35* (right) for three heating/cooling cycles from -40 °C to 200 °C. The upper curves correspond to the heating cycles and the lower curves correspond to the cooling cycles. T_L represents

the liquidus temperature, T_G designates peaks related to glass transitions, T_C and T_2 are the maxima of the cold crystallization in Li30 and Li35, respectively. T_1 and T_3 are the onset of melting and crystallization, respectively.

In Figure 3 a pronounced exothermic peak during heating is located before the melting peak of *Li30, Li25, Li20-2* which indicates cold crystallization. This effect occurs when the supercooled or glassy molten salt becomes sufficiently mobile above the glass transition for crystallisation to occur. The phenomenon is less developed in the field of molten salts but commonly known for complex polymers (e.g. poly ethylene terephthalate (PET)) where it is used to calculate the materials degree of crystallinity.(Wunderlich, 1976) For the intended technical use of the molten salts as heat transfer fluids, at first, it is not considered a significant value. It is also likely that for larger quantities and more impurities supercooling becomes less serve. Yet, if this phenomenon would be confirmed on a larger scale it would become relevant to measure the viscosity of the supercooled liquids at and below 0 °C. For TES and HTF utilization the relevant characteristic value is the liquidus temperature.

From the measurement of a total of 134 compositions, ternary sub-phase diagrams of the tetragonal Ca/K/Na/Li//NO_3 phase diagram were finally obtained and are shown in Figure 4. Each ternary diagram represents a constant Li concentration in the tetragonal quaternary phase diagram (see upper left schematic in Figure 4). Given $LiNO_3$ is the most expensive salt of the quaternary mixture, the Li-contents investigated were limited to maximum 35 % for economic reasons.

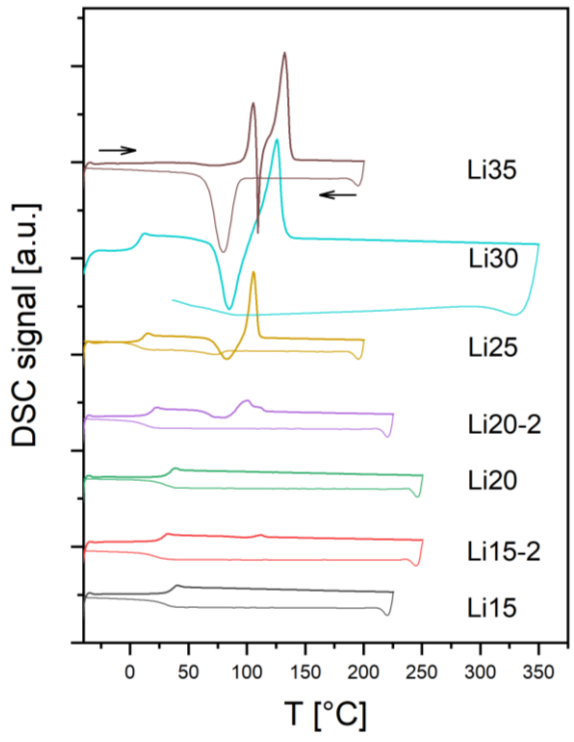

Figure 3. Example of DSC plots during the 3rd heating (upper curve) and cooling (lower part) cycle of 8 molten salt candidates. Data elucidates the presence and absence of melting and crystallization peaks.

In the sub-phase diagram of $(Ca,Na,K)_{0.65}(Li)0._{35}//NO_3$ (Li35, Figure 4, bottom right) all mixtures show non-eutectic melting behaviour from the shape of the melting and/or crystallization curve (not shown). Reducing the Li concentration to 30 mol% (Li 0.3) or 25 mol% (Li 0.25) leads to the formation of

mixtures with lower liquidus temperatures such as *Li30* (T_m~113 °C) or *Li25* (T_m~110 °C), both marked in Figure 4. Those samples represent the lowest melting mixtures for the examined ternary sub-phase diagrams

At concentrations of Li lower than 25 %, supercooling effects are predominant over a large concentration range. Additionally, a large number of samples do not undergo cold crystallization meaning that neither a melting nor a crystallization peak is observed in the DSC measurements. Adapting the sample preparation method by adding crystallization seeds (scratching the crucible bottom or adding small quantities of Al_2O_3-powders) or reducing the measurement temperature to -40 °C was not successful in crystallizing the melt. Salt compositions where no melting or crystallization peak was obtained during the 2nd and 3rd cycle are marked as "glass phase" Figure 4. Nonetheless, from the DSC data of the other compositions it is reasonable to assume that the *real* minimum melting composition of the CaLiNaK system is within those regions of the *Li 0.15* or *Li 0.2* phase diagram marked as "glass phase" in Figure 4.

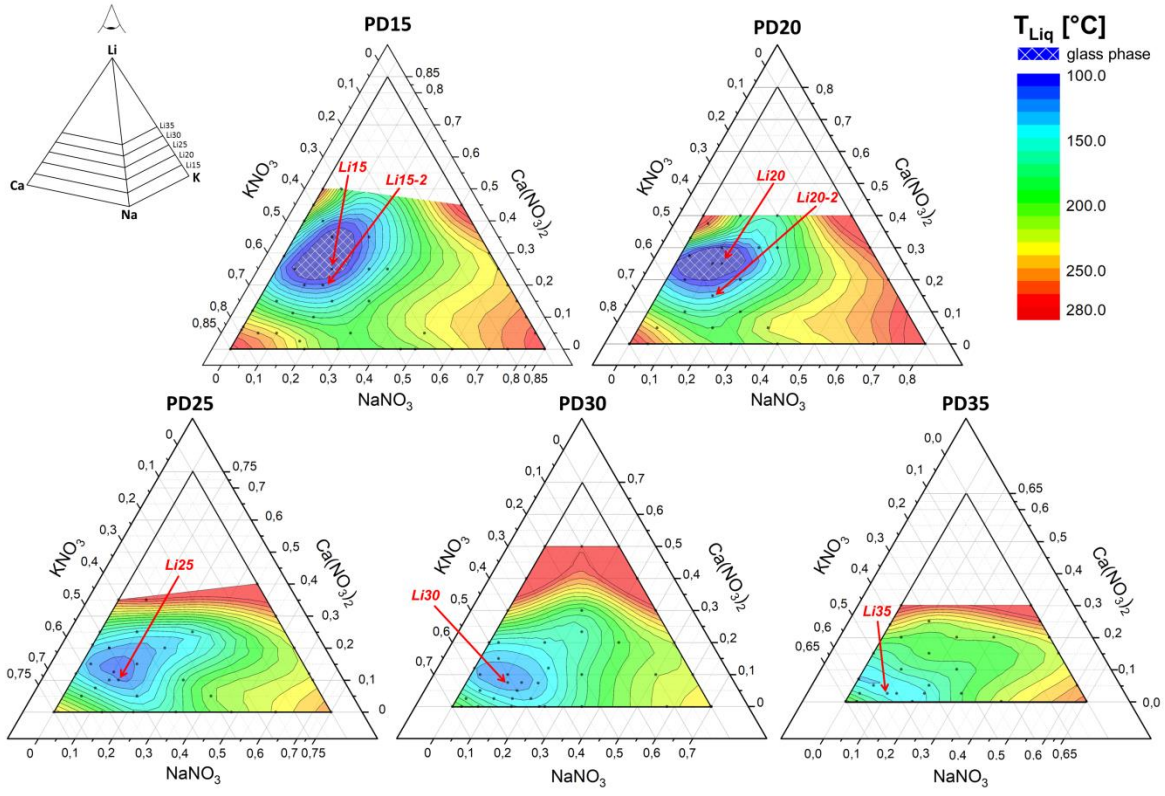

Figure 4. Ternary sub-phase diagrams of the quaternary $LiNO_3$-$Ca(NO_3)_2$-KNO_3-$NaNO_3$ system with different fixed contents of 15, 20, 25, 30 and 35 mol% Li^+, labelled PD15, PD20, PD25, PD30, PD35, respectively. The concentrations of Na, Ca and K are given in mol% and represent the remaining molar fraction in the salt (100 mol% minus Li-content). Data points represent liquidus temperatures extracted from DSC measurements during heating at a rate of 10 K/min. Data points are indicated as black dots. Sides of the ternary diagrams were produced using literature data from Lehrman (Lehrman et al., 1937; Lehrman and Breslow, 1938).

Heat capacity of selected CaLiNaK salts

From a number of compositions the heat capacity was measured since this value is critical for the design of the storage unit, heat exchangers and solar receivers.

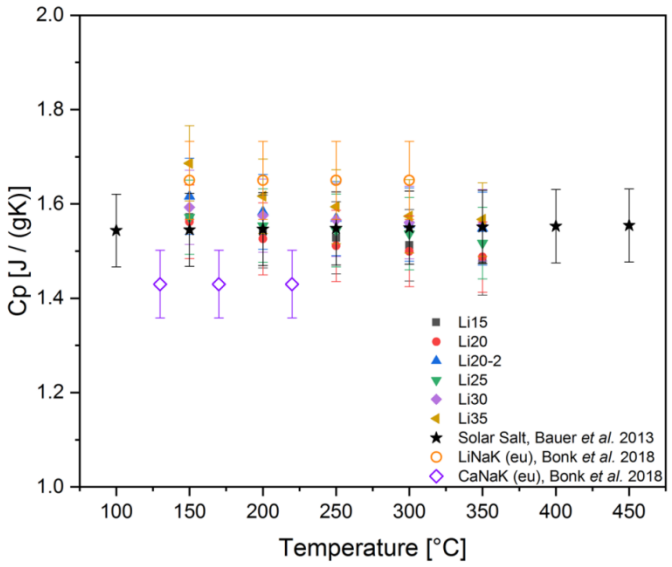

Figure 5. Heat capacity of different CaLiNaK mixtures and literature data from for Solar Salt(Bauer et al., 2013) as well as eutectic LiNaK//NO_3 and CaNaK//NO_3 mixtures (both from ref.(Bonk et al., 2018)). Error bars equal +/-5%.

The C_P data of six quaternary CaLiNaK mixtures is shown in Figure 5 and represents the liquid state of all the samples. The heat capacity of all samples is at or above that of Solar Salt and seems to slightly increase with increasing Li-concentrations. The values also slightly increase at and below 150 °C, which may be due to the close proximity to the endset of the melting peak (e.g. Li35). Moreover, it is important to note that most of the samples exhibit similar heat capacities within the error of measurement of +/- 5 %. The heat capacities are comparable to the values for Solar Salt, but are slightly lower compared to eutectic LiNaK//NO_3 and higher than eutectic CaNaK//NO_3 (both also shown in Figure 5). This follows the trends presented in another review paper published by the authors of this work recently.(Bonk et al., 2018)

The most important thermal properties of the selected molten salt candidates in terms of eutectic, liquidus and crystallization temperature and heat capacity are summarized in Table 4.

Table 4 Eutectic melting temperature (T_{eu}), liquidus temperature (T_{liq}), crystallization temperature ($T_{cryst.}$) and average heat capacity (C_p) (between 150-350 °C) of selected quaternary molten salts. All values were obtained from DSC measurements.

Label	T_{eu}	T_{liq}*	C_{p**}
	[°C]	[°C]	[kJ/kg*K]
Li15	*not detected*	*glassy*	1.527
Li15-2	104.9	116.2	*not measured*
Li20	*not detected*	*glassy*	1.517
Li20-2	92.0	115.7	*not measured*
Li25	99.5	109.8	1.545
Li30	98.4	113.3	1.570

Li35	99.4	136.3	1.608
*: at 10°C/min heating rate ** Average value in the temperature range 150 to 350 °C			

Thermal stability determined by thermogravimetry

The thermal stability of the eight selected CaLiNaK compositions has been qualitatively investigated using TG-analysis followed by additional isothermal experiments discussed in a subsequent paragraph. The TG data during constant heating with 10 K/min is shown in Figure 6. The *T3 method* published by Raade and Padowitz (Raade and Padowitz, 2011) has been used for comparison of all samples and serves purely for qualitative comparison.

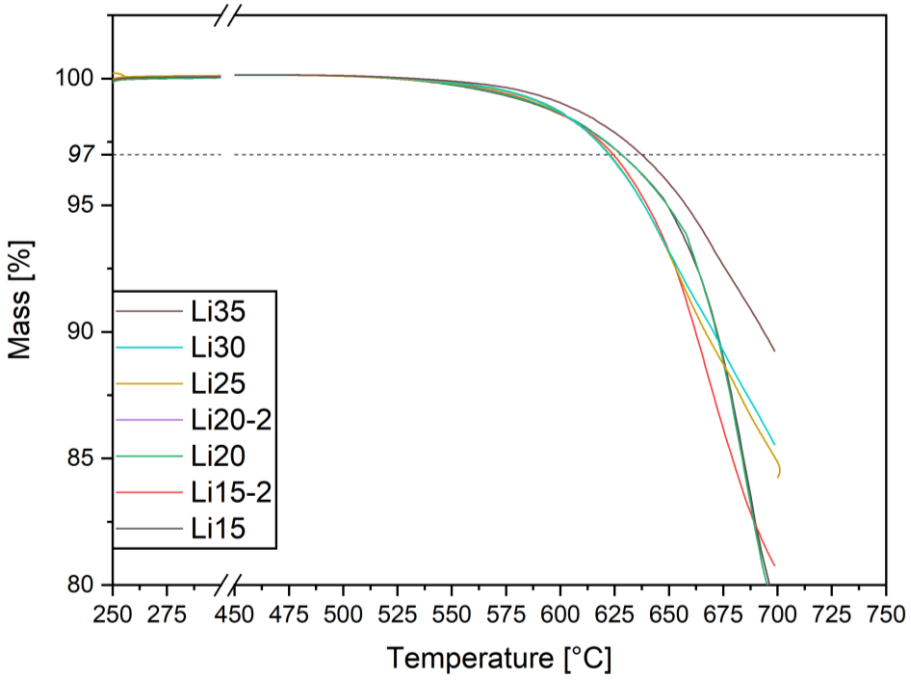

Figure 6. TG curves of 8 CaLiNaK samples during constant heating at 10 K/min.

The mass loss of all samples remains stable up to 500 °C and 3% weight loss is reached between 622 °C and 637 °C making all compositions very comparable in terms of decomposition temperature. Therefore, it can be expected that most samples show similar thermal stability. It has to be emphasized here, that none of the temperatures represent the *real* decomposition temperature and that isothermal experiments are required to elucidate the thermal stability under realistic conditions.

Thermal stability determined by autoclave experiments – the role of anion chemistry

Isothermal stability experiments in the 100 g-scale were complemented by chemical post-analysis of extracted molten salt samples in terms of anion and cation compositions. All results are compared to the composition of a pure Solar Salt batch performed under the same conditions. During the 500 h-experiments at 500 °C samples were extracted when reaching the operating temperature (at t = 0 h) and after 72, 120, 240, 400 and 500 h. After opening the autoclave system, it was immediately

obvious that all the CaLiNaK mixtures appeared to be more heterogeneous than the Solar Salt sample. A top view into the alumina crucible with a representative *Li20-2* sample after the experiment is shown in Figure 7 (a). The heterogeneity of the sample indicates that decomposition reactions were much more pronounced than in the Solar Salt sample, an image of which is shown in Figure 7 (b). Moreover, it could be observed that all CaLiNaK samples creeped up the walls of the alumina crucible and turned yellowish (see Figure 6 left). Consequently, an additional yellowish salt sample was extracted from the fraction that creeped up the walls, which will hereafter be referred to as *Creep Salt*.

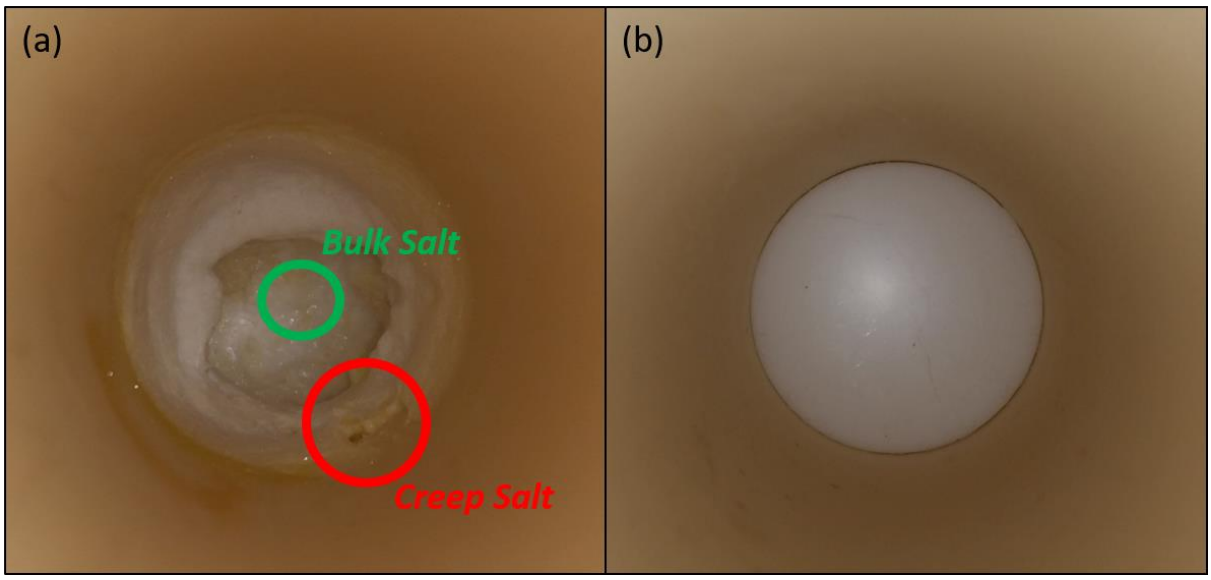

Figure 7. Image at room temperature of solidified molten salts after 500 h at 500 °C: (a) the *Li20-2* sample and (b) the Solar Salt sample. The salt fractions referred to as "Creep Salt" and "Bulk Salt" throughout this manuscript are indicated in (a).

The anion chemistry in terms of nitrate, nitrite and oxide ions is shown in Figure 8 as opposed to the reference Solar Salt sample. In Solar Salt, a nitrate-nitrite equilibrium establishes with 95.3 mol% nitrate and ~4.5 mol% nitrite and only minor quantities of oxide ions (< 0.1 mol%). .

For the CaLiNaK samples after 500 h different results in terms of anion compositions are obtained. While most samples exhibit similar nitrite levels between 3.29 and 5.18 mol%, oxide ion levels and nitrate levels vary significantly. The highest concentrations of oxide ions are found in *Li15-2* (8.35 mol%) and *Li20* (11.52 mol%), which gives rise to excessive decomposition reactions, most likely according to eq. (2). At the same time the nitrate levels are significantly below that of Solar Salt at 86.9 mol% and 83.7 mol%, respectively. We assume that the first reaction is the formation of a nitrate-nitrite equilibrium. The nitrite ion further decomposes to form the oxide ions along with the formation of nitrous gases. The constant removal of nitrous gases with the purge gas flow pushed the equilibrium of reaction (2) to the product (oxide ion) side. Simultaneously, the nitrite concentration remains stable due to the further decomposition of the nitrate ions according to equilibrium reaction (1). The latter can mainly be attributed to the constant oxygen partial pressure in the purge gas (0.2 atm O_2) which leads to

a steady regeneration of the otherwise decomposing nitrite ion. All of which leads to decreasing nitrate-, increasing oxide ion- and stable nitrite levels.

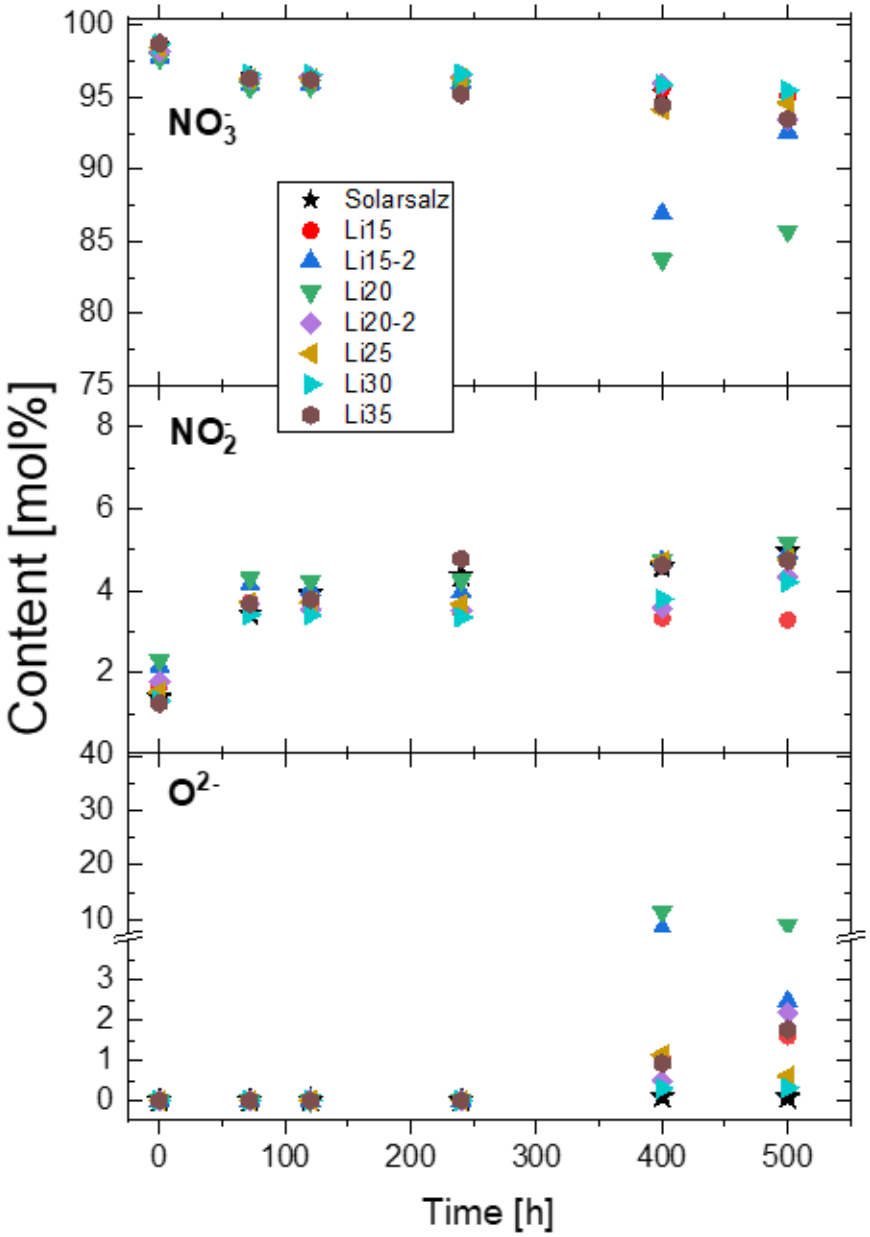

Figure 8. Anion composition of (left) the bulk fractions of the CaLiNaK mixtures extracted throughout the 500 °C-experiment and (right) the *CreepSalt* extracted after the end of the experiment. Note the different y-axis in the left and right graphs.

For the samples *Li15*, *Li20-2*, *Li25* and *Li35* the oxide levels were lower (1-2 mol%) compared to the other CaLiNaK samples, but still significantly higher than in Solar Salt.

The samples *Li15-3* and *Li35* with the lowest Ca amount show the overall lowest oxide ion concentrations of all CaLiNaK samples which may give rise to a more stable anion chemistry. When however, looking at the *CreepSalt* of the samples, a significantly higher oxide ion fraction and lower

nitrate and nitrite fraction are identified compared to the bulk salt (Figure 8 (right)). For all CaLiNaK samples this indicates that demixing phenoma occur during the isothermal experiment. It is reasonable to assume that this effect is caused by salt creeping up the crucible walls which then decomposes to a much greater extent than the bulk fraction. The oxide ion concentration in the CreepSalt reaches high values up to 50 mol% in some cases, indicating that it decomposes to a higher extent than the bulk salt.

In the next paragraph the observations made so far are complemented with cation analyses which allow for a more detailed assessment of the thermal stability limit in depth.

Effects of cation chemistry on thermal stability

The concentration of Li, Na, K and Ca-cations in the extracted salt samples was analysed using cation chromatography. The calcium content in the bulk fraction of the molten salts, plotted in in Figure 9 (a), was subject to steady changes over time decreases steadily over time while the Na-, K- and Li-content increase simultaneously (see Figure S 1). After finishing the isothermal stability tests, the CreepSalt was found to contain drastically increased concentrations of calcium. All of which indicated that Ca is selectively removed from the molten salt bulk and diffused towards the walls of the crucible where it was steadily enriched.

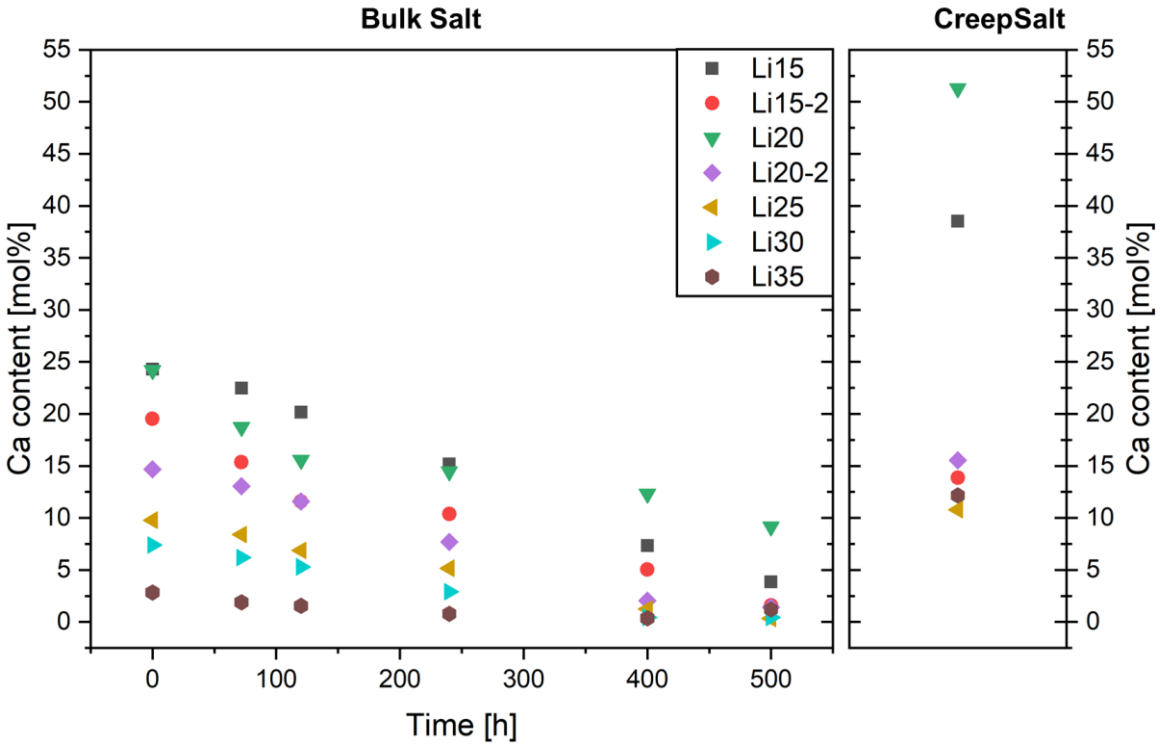

Figure 9 Molar Ca content (left) in the extracted bulk fraction of the molten salt and (right) the *CreepSalt* extracted after the end of the experiment.

Together with the selective enrichment of oxide ions in the *CreepSalt* it is reasonable to assume the following decomposition process. For each of the CaLiNaK salts a fraction of the salt creeps up the crucible walls leading to an increasing surface area. Given the larger surface area kinetics of the

decomposition reactions are enhanced. The molten salt partially decomposes into nitrite and oxide ions with the release of oxygen and nitrous gases. Due to the constant removal of the nitrous gases with the purge gas oxide ions can accumulate in the *CreepSalt*. We assume, that after reaching a critical (yet unknown) concentration of oxide ions, the precipitated as CaO at the crucible walls. It has to be noted that this is based on the observation that oxides of calcium exhibit a lower solubility than those of Li, Na or K. Eventually, the precipitation of calcium oxide compounds leads to a concentration gradient, which leads to diffusion of calcium ions from the bulk salt towards the CreepSalt. Thereby, Ca is constantly depleted from the bulk and accumulates as solid CaO-rich phase on the walls of the crucible.

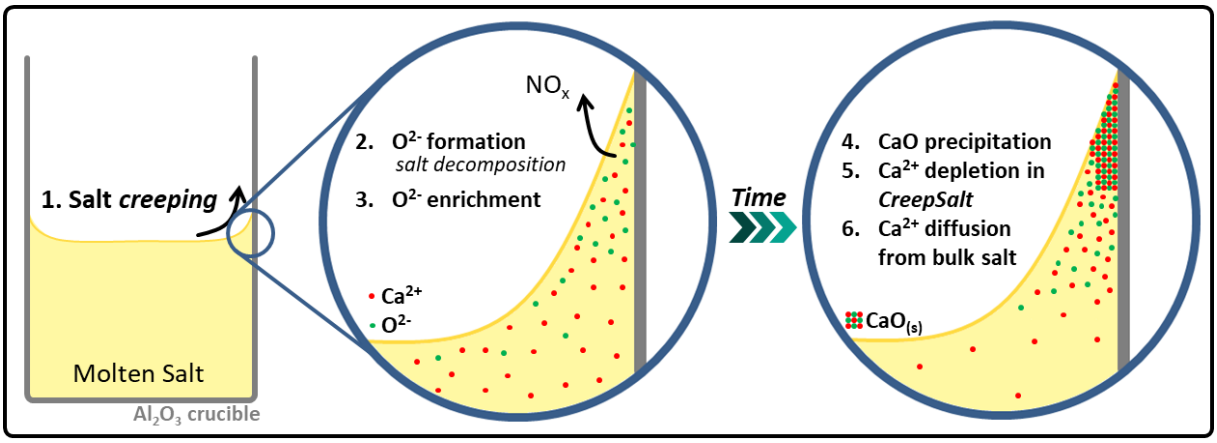

Figure 10 Reaction scheme of the decomposition of CaLiNaK molten salt mixtures with calcium oxide enrichment in the CreepSalt.

This behavior is especially pronounced for samples with high initial Ca-contents such as e.g. *Li20* and *Li15* (both 25% Ca^{2+}), while it is less pronounced for *Li35* (2.5% Ca^{2+}) as shown in Figure 8 on the right. The *Li35* salt shows a constant nitrate, nitrite and oxide level in the bulk fraction and the lowest CaO content in the *CreepSalt*, making it the most stable salt candidate amongst the CaLiNaK-compositions tested. Overall, these autoclave results are in good agreement with the TG analysis results, where *Li35* showed the highest decomposition temperature of all samples.

Overall, the stability of the CaLiNaK samples highly depends on the Ca concentrations which seems to trigger decomposition reactions due to the formation of oxide compounds with low solubility. This effect is of course very pronounced when investigating a few 100g of sample since the surface-to-volume ratios are higher than in the kg- or ton-scale. Nonetheless, it has to be noted that changes in the salt composition not only may lead to the formation of insoluble oxide ions, but also affect the salt composition and thereby its thermo-physical properties. In particular, one can expect that the melting point of the salt increases with ongoing Ca-depletion and thereby reduces the applicable ΔT.

Conclusions

The work presented investigates the minimum melting mixtures of the quaternary Ca/K/Na/Li//NO_3 system. Ternary subsystems of the $(CaNaK)_{1-x}Li_x$ //NO_3 – type were measured for Li concentrations of

between 15 – 35 mol%. From more than 130 DSC measurements the low-melting regions of the ternary sub-systems were assessed but eutectic compositions could not be identified due to severe supercooling effects. The *Li25* mixture (10-52.5-12.5-25 mol% Ca-K-Na-Li) exhibited the lowest liquidus temperature of 109.8 °C at a heating rate of 10 K/min.

The temperature dependent heat capacity of all samples appeared to increase with increasing Li-concentrations which agreed well with available literature data. Nonetheless, differences amongst samples were typically within the error of measurement and almost temperature independent values of 1.52 – 1.61 J/gK were obtained between 150-350 °C.

Thermal analysis data revealed that all samples exhibit a very similar decomposition temperature (3% weight loss-method) between 622 °C – 664 °C. No trend in terms of stability was observed throughout the different salt compositions. Analysis of the molten salt chemistry revealed decomposition reactions which were specific to the presence of Ca in the melt and linked to salt creeping phenomena. These phenomena led to the formation of presumably solid CaO phases towards the top of the crucible leading to steady Ca-depletion of the bulk salt. Both effects were attributed to salt creeping along hot walls of the crucible, followed by decomposition reactions and successive precipitation of low-solubility-CaO phases. Reactions could be supressed in mixtures containing low concentrations of Ca such as *Li35* (T_{liq}: 136 °C; Ca-K-Na-Li: 2.5-52.5-10-35 mol%), which showed the best thermal performance of all samples tested. The results of our study provide a pathway for the synthesis of low-melting point molten salts and also contributes to a deeper understanding of decomposition mechanisms in molten salts.

Acknowledgements

We thank Stefan Wohnrau for performing DSC analysis, assistance with thermal stability tests and Andrea Hanke for assisting with ion chromatography.

References

ASTM E794 - 06: Standard Test Method for Melting And Crystallization Temperatures By Thermal Analysis.

2004. Comprehensive Handbook of Calorimetry and Thermal Analysis. John Wiley & Sons Ltd.

2017. ASTM E1269-11, Standard Test Method for Determining Specific Heat Capacity by Differential Scanning Calorimetry.

Ahmad, N.N.B., Yunos, N.B., Muhammad, W.N.A.B.W., Mohamad, M.N.A.B., Yusof, F.B., 2017. Effect of lithium nitrate and calcium nitrate composition on the thermal properties of quaternary molten salts mixture for heat transfer application. Journal of Physics: Conference Series 914, 012027-012027.

Bale, C.W., Bélisle, E., Chartrand, P., Decterov, S.A., Eriksson, G., Gheribi, A.E., Hack, K., Jung, I.H., Kang, Y.B., Melançon, J., Pelton, A.D., Petersen, S., Robelin, C., Sangster, J., Spencer, P., Ende, M.A.V., 2016. FactSage thermochemical software and databases, 2010–2016. Calphad 54, 35-53.

Baraka, A., I. Abdel-Rohman, A., A. El Hosary, A., 1975. Corrosion of Mild Steel in Molten Sodium Nitrate-Potassium Nitrate Eutectic. British Corrosion Journal 11, 44-46.

Bauer, T., Pfleger, N., Breidenbach, N., Eck, M., Laing, D., Kaesche, S., 2013. Material aspects of Solar Salt for sensible heat storage. Applied Energy 111, 1114-1119.

Bergman, A.G., Rassonskaya, I.S., Shmidt, N.E., 1955. Izvest. Sektora Fiz.-Khim Anal. 26, 156-156.

Berul, S.I., Bergman, A.G., 1954. Izvest. Sektora Fiz.-Khim Anal. Akad. Nauk S.S.S.R.

Bond, B.D., Jacobs, P.W.M., 1966. The thermal decomposition of sodium nitrate. Journal of the Chemical Society A: Inorganic, Physical, Theoretical, 1265-1265.

Bonk, A., Braun, M., Sötz, V.A., Bauer, T., 2020. Solar Salt – Pushing an old material for energy storage to a new limit. Applied Energy 262, 114535.

Bonk, A., Martin, C., Braun, M., Bauer, T., 2017. Material Investigations on the Thermal Stability of Solar Salt and Potential Filler Materials for Molten Salt Storage. AIP Conference Proceedings 1850, 080008: 080001-080008-080008.

Bonk, A., Rückle, D., Kaesche, S., Braun, M., Bauer, T., 2019. Impact of Solar Salt aging on corrosion of martensitic and austenitic steel for concentrating solar power plants. Solar Energy Materials and Solar Cells 203.

Bonk, A., Sau, S., Uranga, N., Herainz, M., Bauer, T., 2018. Advanced heat transfer fluids for direct molten salt line-focusing CSP plants. Progress in Energy and Combustion Science 67C, 69-87.

Bonk, A., Sötz, V., Bauer, T., Molten Salt Chemistry in the Lab- & MW-Scale – Operational Experiences from the Molten Salt Storage Facility TESIS at DLR.

Bradshaw, R.W., 2010. Viscosity of multi-component molten nitrate salts - Liquidus to 200°C.

Carveth, H.R., 1898. Study of a Three-Component System. The Journal of Physical Chemistry 2(4), 209-228.

Cordaro, J.G., Bradshaw, R.W., 2010. Low-Melting Point Heat Transfer Fluid. Sandia Corporation, Livermore, CA, United States of America.

Delise, T., Tizzoni, A.C., Ferrara, M., Corsaro, N., D'Ottavi, C., Sau, S., Licoccia, S., 2019. Thermophysical, environmental, and compatibility properties of nitrate and nitrite containing molten salts for medium temperature CSP applications: A critical review. Journal of the European Ceramic Society 39(1), 92-99.

Donato, G., Belongie, S., 2002. Approximate Thin Plate Spline Mappings, in: Heyden, A., Sparr, G., Nielsen, M., Johansen, P. (Eds.), Computer Vision — ECCV 2002. Springer Berlin Heidelberg, Berlin, Heidelberg, pp. 21-31.

Fernández, A.G., Ushak, S., Galleguillos, H., Pérez, F.J., 2014. Development of new molten salts with LiNO3 and Ca(NO3)2 for energy storage in CSP plants. Applied Energy 119, 131-140.

Glatzmaier, G., Siegel, N.P., 2010. Molten salt heat transfer fluids and thermal storage technology.

Gomez, J.C., Calvet, N., Starace, A.K., Glatzmaier, G.C., 2013. Ca(NO3)2 - NaNO3 - KNO3 Molten Salt Mixtures for Direct Thermal Energy Storage Systems in Parabolic Trough Plants. Journal of Solar Energy Engineering 135(2), 021016-021016.

González-Roubaud, E., Pérez-Osorio, D., Prieto, C., 2017. Review of commercial thermal energy storage in concentrated solar power plants: Steam vs. molten salts. Renewable and Sustainable Energy Reviews 80(Supplement C), 133-148.

Kirst, W.E., Nagle, W.M., Castner, J.B., 1940. A New Heat Transfer Medium for High Temperatures. Transactions of the American Institute of Chemical Engineers 36, 371-394.

Kofler, A., 1955. Mikrothermoanalyse des Systems NaNO3-KNO3. Monatshefte für Chemie und verwandte Teile anderer Wissenschaften 86(4), 643-652.

Kuravi, S., Trahan, J., Goswami, D.Y., Rahman, M.M., Stefanakos, E.K., 2013. Thermal energy storage technologies and systems for concentrating solar power plants. Progress in Energy and Combustion Science 39(4), 285-319.

Lehrman, A., Adler, E., Freidus, J., Neimand, M., 1937. The Liquidus Curve and Surface of the Systems Lithium and Calcium Nitrates and Calcium, Lithium and Potassium Nitrates. Journal of the American Chemical Society 59(1), 179-181.

Lehrman, A., Breslow, D., 1938. The Liquidus Surface of the System Sodium, Lithium and Calcium Nitrates. Journal of the American Chemical Society 60(4), 873-876.

Lehrman, A., Selditch, H., Skell, P., 1936. The Binary System Potassium Dichromate—Sodium Dichromate. Journal of the American Chemical Society 58(9), 1612-1615.

M. De Jong, J., H. J. Broers, G., 1976. A reversible oxygen electrode in an equimolar KNO3-NaNO3 melt saturated with sodium peroxide - II. A voltammetric study. Electrochimica Acta 21, 893-900.

Muñoz-Sánchez, B., Nieto-Maestre, J., González-Aguilar, J., Julia, J.E., Navarrete, N., Faik, A., Bauer, T., Bonk, A., Navarro, M.E., Ding, Y., Uranga, N., Veca, E., Sau, S., Giménez, P., García, P., Burgaleta, J.I., 2017. Round Robin Test on the Measurement of the Specific Heat of Solar Salt. AIP Conference Proceedings 1850(1), 080017-080011--080017-080018-080017.

Olivares, R.I., 2012. The thermal stability of molten nitrite/nitrates salt for solar thermal energy storage in different atmospheres. Solar Energy 86(9), 2576-2583.

Origin(Pro), 2018 ed. OriginLab Corporation, Northampton, MA, USA.

Protsenko, P.I., Bergman, A.G., 1950. Binary System KNO3-Ca(NO3)2. Zh. Obshch. Khim. 20, 1365-1375.

Protsenko, P.I., Medvedev, B.S., 1963a. The Ca,Na//NO2,NO3 System. Russian Journal of Inorganic Chemistry 8(12), 1434-1436.
Protsenko, P.I., Medvedev, B.S., 1963b. The Li,Na//NO2,NO3 System. Russian Journal of Inorganic Chemistry 8(12), 1436-1438.
Protsenko, P.I., Shisholina, R.P., 1963. The K,Li // NO2, NO3 System. Russian Journal of Inorganic Chemistry 8(12), 1438--1441.
Raade, J.W., Padowitz, D., 2011. Development of Molten Salt Heat Transfer Fluid With Low Melting Point and High Thermal Stability. Journal of Solar Energy Engineering 133(3), 031013-031013.
Reddy, V.S., Kaushik, S.C., Ranjan, K.R., Tyagi, S.K., 2013. State-of-the-art of solar thermal power plants - A review. Renewable and Sustainable Energy Reviews 27, 258-273.
Ren, N., Wu, Y.-t., Ma, C.-f., Sang, L.-x., 2014. Preparation and thermal properties of quaternary mixed nitrate with low melting point. Solar Energy Materials and Solar Cells 127, 6-13.
Roozeboom, H.W.B., 1904. Die heterogenen Gleichgewichte vom Standpunkt der Phasenlehre, zweites Heft. Systeme aus zwei Komponenten. Erster Teil. Friedrich Vieweg.
Siegel, N.P., Cordaro, J.B., Bradshaw, R.W., Kruizenga, A.M., Thermophysical Property Measurement of Nitrate Salt Heat Transfer Fluids, Proceedings of the ASME 2011 5th International Conference on Energy Sustainability. pp. 54058--54051 - 54058-54058-54058.
Sötz, V.A., Bonk, A., Forstner, J., Bauer, T., 2018. Molten salt chemistry in nitrate salt storage systems: Linking experiments and modeling. Energy Procedia 155, 503-513.
Stern, K.H., 1972. High Temperature Properties and Decomposition of Inorganic Salts - Part 3 Nitrates and Nitrites. Journal of Physical and Chemical Reference Data 1(3), 748-772.
Vignarooban, K., Xu, X., Arvay, A., Hsu, K., Kannan, A.M., 2015. Heat transfer fluids for concentrating solar power systems: A review. Applied Energy 146(Supplement C), 383-396.
Wunderlich, B., 1976. Macromolecular Physics. Volume 2: Crystal Nucleation, Growth, Annealing. Academic Press.
Yu-ting, W.U., Ying, L.I., Yuan-wei, L.U., Wang, H.-f., Chong-fang, M.A., 2017. Novel low melting point binary nitrates for thermal energy storage applications. Solar Energy Materials and Solar Cells 164, 114-121.
Yuvaraj, S., Fan-Yuan, L., Tsong-Huei, C., Chuin-Tih, Y., 2003. Thermal Decomposition of Metal Nitrates in Air and Hydrogen Environments. Journal of Physical Chemistry B 107, 1044-1047.
Zambonin, P.G., 1973. Oxides/oxygen systems in molten alkali nitrates: Remarks and hypotheses concerning recent literature findings. Journal of Electroanalytical Chemistry and Interfacial Electrochemistry 45(3), 451-458.

Supplementary Material

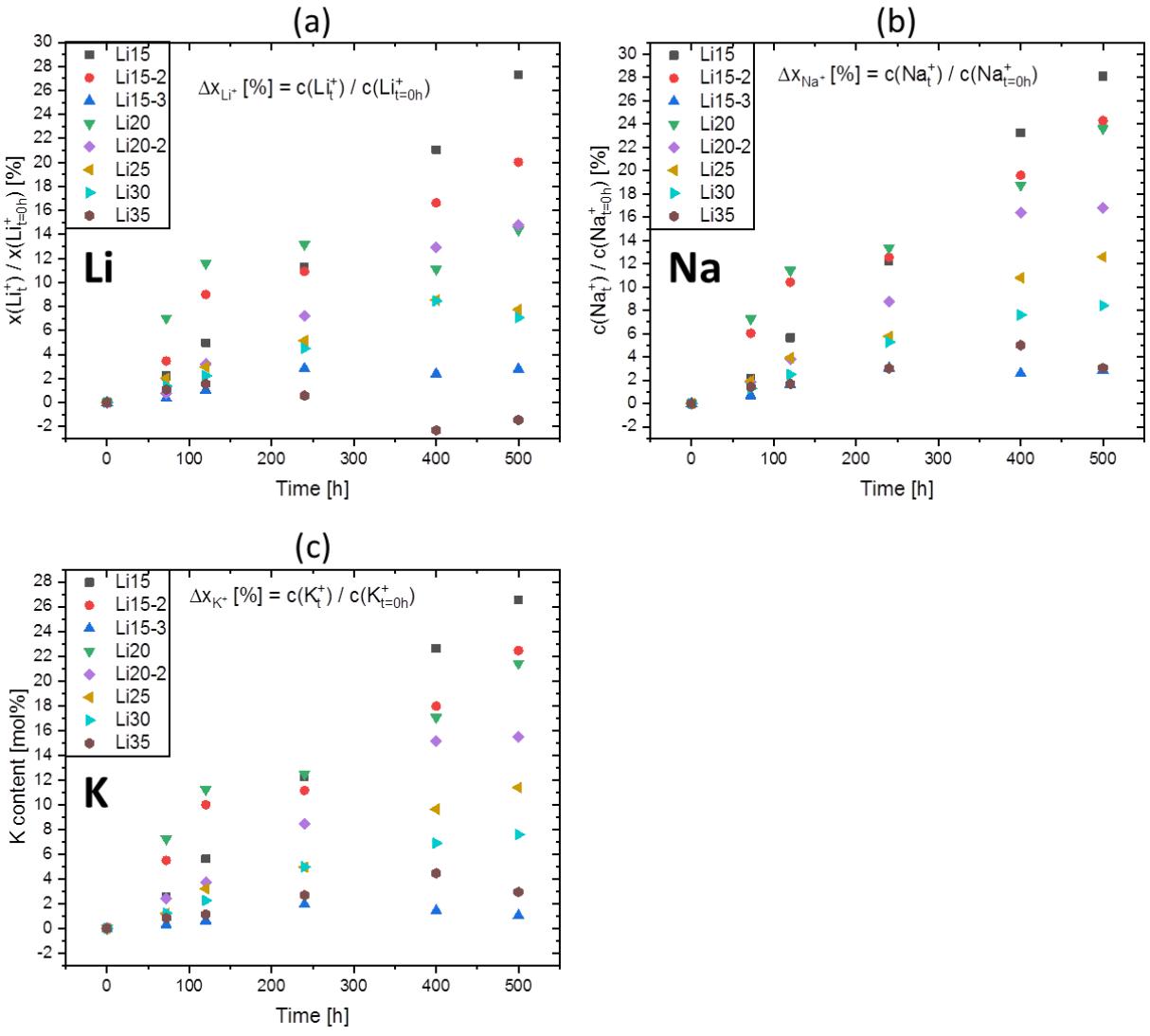

Figure S 1 Relative changes in cation contents of (a) Li, (b) Na and (c) K in the bulk fraction of the molten CaLiNaK salts during isothermal storage experiments. Values are calculated from the concentration of the cation at a given point in time divided by the concentration at the start of the experiment (t = 0h).